

# On Self-adjusting Contacts in Pin-On-Disk Testers

Alexander Vogel<sup>1</sup>, Georg-Peter Ostermeyer<sup>2</sup>

*Technische Universität Braunschweig, Institute of Dynamics and Vibrations  
Schleinitzstr. 20, 38106 Braunschweig, Germany (E-mail: <sup>1</sup>alexander.vogel@tu-bs.de; <sup>2</sup>gp.ostermeyer@tu-bs.de)*

<https://doi.org/10.46720/EB2020-STP-044>

**ABSTRACT:** The Automated Universal Tribotester (AUT) represents a fully automated reduced scale brake dynamometer. The setup is based on the pin-on-disc principle, where the specifically designed load unit, on the one hand, guides the pin and on the other hand applies the necessary normal load on the friction contact. Even with highly developed tribometers such as the AUT at IDS, long bedding processes after load changes are necessary for a valid evaluation of wear and emissions. The applied loads in combination with the limited material stiffness of machines result in an inevitable tilting of the pin, which influences the surface dynamics in the friction layer. Only an intelligent adaptive compensation system is capable of measuring and adjusting the specimen's alignment towards the disc during measurements in a way, that a full surface contact can be assured. This paper presents the adaptive system, which is added to the load unit of our fully automated tribometer. It presents the observer model to monitor the specimen's angle in the friction interface, including its application in the overall control loop. Furthermore, the kinematic principle with its self-locking features and the drive concept is presented. Finally, this paper demonstrates the adjustment range and speed performance of the complete adaptive system. The impact of the compensation on characteristic values of friction such as the coefficient of friction, wear and emissions will be presented elsewhere.

**KEYWORDS:** Pin on disk, self-adjusting, misalignment, tilting, wear, emission.

## 1. Introduction

The need for a prediction of wear and emissions in brakes gains rapidly in importance. For this purpose, the Ostermeyer friction model for the dynamic coefficient of friction [1] will be extended in the future towards the dynamic description of wear and the emission of particles. For parameter fitting and validation, a highly capable tribometrical test stand is necessary to meet the requirements for highly time-resolved and precise measurements [2].

It is capable to handle various test materials, e.g. full-size brake disks and sample cutouts from commercial brake pads. The central part of this tribometer is the load unit (Figure 2), which combines the tasks of applying the normal load, guiding the pin in the contact and withstanding the occurring friction loads. This includes the friction force and also thermal loads and wear particles polluting the test stand. Speeds and forces can be dynamically varied to simulate various friction scenarios and topography measurements can be conducted intermittently [3, 4, 5].

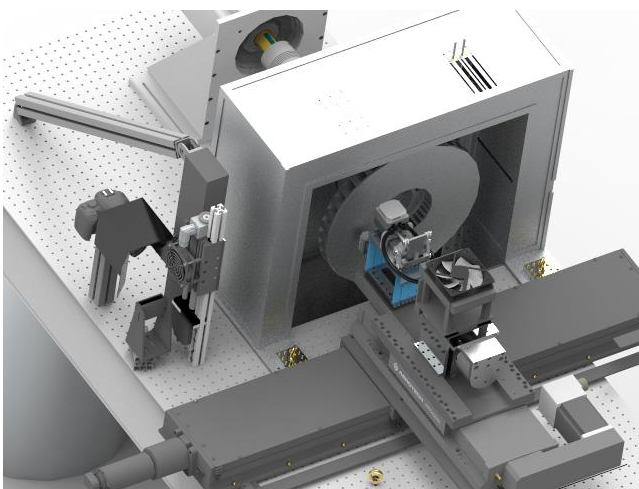


Figure 1: Automated Universal Tribometer at TU Braunschweig

The Automated Universal Tribotester (AUT) (Figure 1) is a technologically advanced and fully automated tribometer with a pin

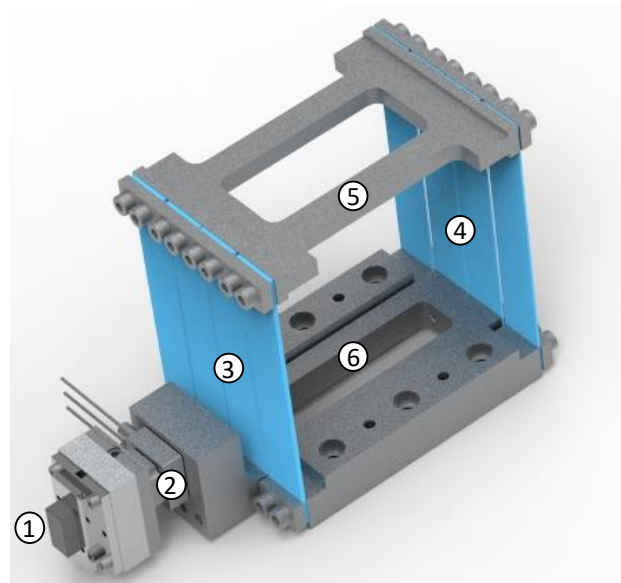


Figure 2: Load Unit of the AUT: brake pad sample facing the disc (1), force sensor (2), front (3) and rear (4) leaf springs, top bridge (5) and bottom bridge (6)

Frequent changes in the load spectrum (e.g. normal load or sliding speed) induce in turn frequent changes in the load on the tribometer and its load unit in particular, tilting the friction interface and avoiding a full contact. Great efforts were taken to optimize the geometrical design of the load unit to have optimal passive compensation for those effects [6]. Passive optimizations are limited to a specific load case, and due to the limited material stiffness of any material, full compensation can not be achieved [7]. This is a problem that every pin on disk tester has, and the magnitude and effects depend on the specific design (compare [8, 9, 10, 11]).

The proposed solution in [7] consists of a stepper motor moving the rear springs of the load unit and thus lifting the bottom bridge (Figure 2, Item 6) to induce a counter angle to the test specimens surface. This approach was functional but was since then improved in terms of angular range, adjustment speed, and applicable load. Besides, an Observer Model was implemented to determine the actual angle of the specimen's surface based on the measured forces, which will also be presented in this paper.

## 2. Mechanical Design

The mechanical linkage between the stepper motor and the springs is the key element to manipulate the characteristics of the tilting motion. The angular adjustment has to be fast, precise, and powerful enough to face the occurring normal and friction forces.

Since the motor is limited in size and thus in its power, a mechanical linkage is needed to scale the forces of the motor to match the requirements of the friction measurements. To increase the speed of the actuation, the connection between the stepper motor and the leaf springs has to be direct in comparison to the previous setup. This is achieved by a sole vertical movement of the rear springs, which are linked to the central beam carrying the test specimen. The front leaf springs then act as a hinge, forcing the motion into a circular movement (Figure 3) and resulting in the residual angle  $\beta$  between the surface of the pad and the disc.

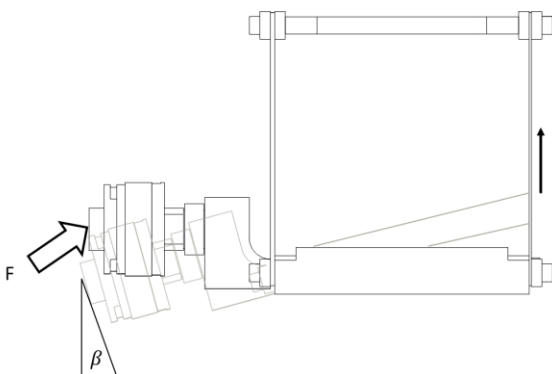


Figure 3: Direct actuated mechanism to tilt the test specimen

A stepper motor matches the properties perfectly that are needed for the adaptive system. It has a high holding torque and nearly full torque from a standstill, enabling the necessary accelerations during

operation. In combination with a trapezoidal spindle and the right thread pitch, the drive system is self-locking in case of motor failure.

The connection between the rear leaf springs and the actuator on top of the load unit needs to be a mechanical linkage with the transmission of force. A force ratio between the stepper motor output and the occurring maximum forces during friction measurements was estimated to approximately 1:3.8. Also, an exclusive vertical linear motion is necessary to keep the effects of the adjustment on the normal force small, since any horizontal movements of the springs would reduce the applied target load.

Many mechanisms with sole linear motion are complex and consist of several linkage bodies (e.g. Kempe- or Peaucellier- mechanisms) or have only an approximate linear motion (e.g. Watt-, Tchebychev- or Hoecken- mechanisms). The solution that combines exact linear vertical motion with simplicity is the symmetrical crankshaft (Figure 4).

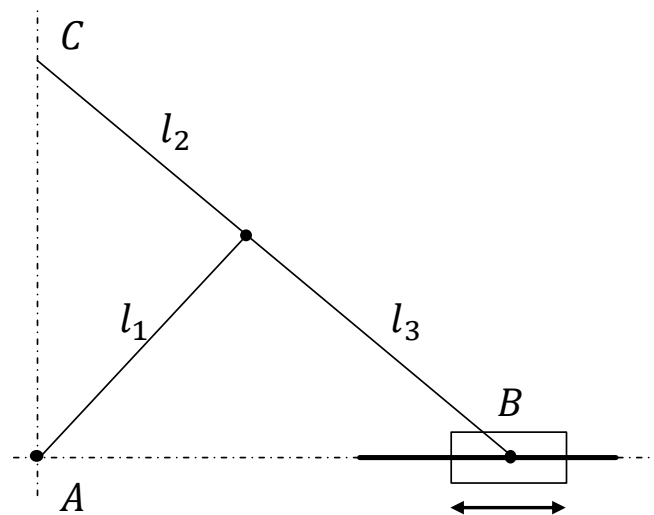


Figure 4: Symmetrical crankshaft with  $l_1 = l_2 = l_3$  and exact linear vertical motion of point C and exact linear horizontal motion of point B

The final design comprises a symmetrical setup of the crankshafts to withstand lateral motions and to increase stability. The whole assembly is illustrated in Figure 5. The actuator assembly includes the main parts stepper motor, linear stage, and the crankshafts, and it is mounted on top of the load unit and connected to the rear leaf springs.

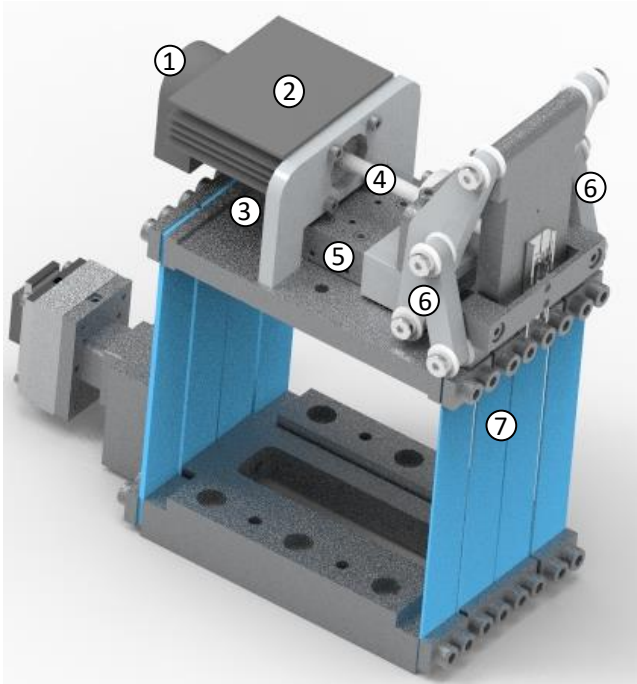


Figure 5: Final design of the adaptive actuator with encoder (1), a passive heat sink (2), stepper motor (3), rotary shaft (4), linear stage (5), symmetrical crankshaft (6) and rear leaf springs that are actuated (7)

### 3. Electric Components

The electrical system besides the stepper motor and the encoder is placed in a central control box. This box is powered by an AC power supply and supplies all electric components. Its central computer is a microcontroller based on Arduino, which is controlling the whole adaptive system. It can also be remotely accessed by a PC to set control parameters or to record data.

The stepper motor is powered by the stepper motor driver, which in turn receives the commands from the Arduino. For initial setups and measuring the specimens angle and forces, additional sensors can be connected. Angular sensors will not be needed in the future since a software-based sensor is applied for friction measurements. The whole system can be monitored and operated via the HMI-Interface with an LCD screen and buttons to navigate the menus. An overview of the information and energy connection is illustrated in Figure 6.

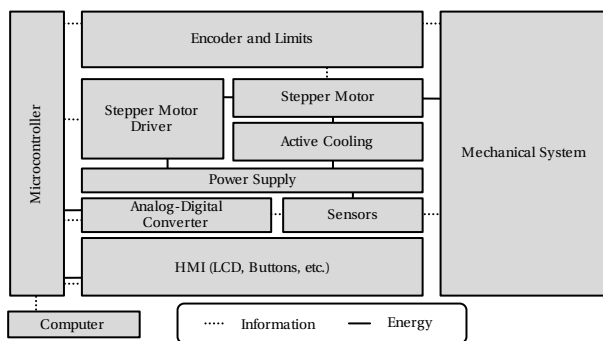


Figure 6: Information and energy flow in the electrical system

On startup, the program follows an initial boot/setup routine before the menus are available (Figure 7). This is necessary to initialize the stepper motor to acquire its absolute position via the limit switches.

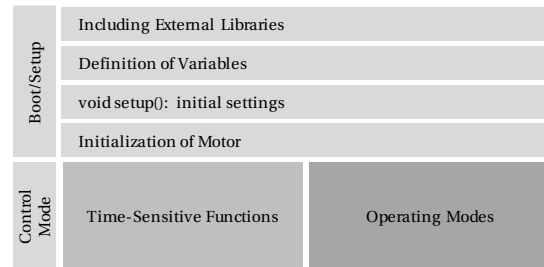


Figure 7: Process diagram of the internal software on the Arduino

The automatic mode is applicable for the usual friction measurements and is loaded automatically after booting. Other modes are available for the acquisition of characteristic curves of the setup or for adjusting and debugging and include a speed and position mode.

Time-sensitive functions are accessed on the schedule of a timer on the Arduino to guaranty their precise execution. The highest priority has the update function and error handling of the stepper motor to ensure that the motor moves as quickly as possible if a step is due. This is followed by a high and controlled sample rate of the force sensors. The data is then saved in a ring buffer and filtered before it is further processed. Low-frequency functions are the communication to the computer, updating the HMI and reading temperature values.

### 4. Observer Model and Implementation

The angle  $\beta$  is the residual angle between the test specimen surface and the brake disc. It is supposed to be zero to ensure full surface contact in the friction layer. It is on the one hand caused by the applied load spectrum on the friction contact as a function of normal force and tangential force  $f(F_N, F_T)$ , and on the other hand as a counter-angle induced by the actuators position  $f(s)$  (equation 1).

$$\beta = f(F_N, F_T) + f(s) \quad (1)$$

Both functions need to be determined and solved during the friction measurements to output the actual residual angle as the input for the control model. Based on this value, the control system adjusts the motor speed to reduce the error to the setpoint (here zero degrees), compare Figure 8.

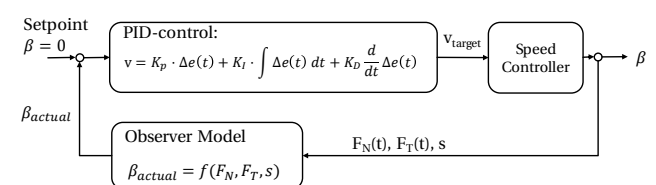


Figure 8: Control diagram for the stepper motor and implementation of Observer Model

The controller calculates the error  $e$  between setpoint  $\beta$  and the actual angle of the specimen  $\beta_{actual}$ , which is then used to calculate a necessary target speed to minimize the error. Realizing the target speed with the stepper motor is the task of the stepper motor driver. Measured forces in the normal direction ( $F_N$ ) and tangential direction ( $F_T$ ) and the actual actor position are acquired at the end of the time step and made available to the implemented Observer Model.

Determination of the function  $f(s)$ , which connects the actor position to the actor-induced counter angle, is achieved by measurements of the real system. The system characteristics can be very well approximated with a polynomial of second degree. The coefficients are given in Table 1.

Table 1: Coefficients for the fitting of  $f(s)$

$a_0$	0.548524
$a_1$	0.000386
$a_2$	2.09317e-08

Under load, the load unit deflects and brings an unwanted angle and misalignment into the test setup. This deflection can be approximated with a beam model of the form of equation 2.

$$\alpha_F(x_2) = -\frac{1}{EI} \left( \frac{1}{2} F_T x_2^2 + (F_N e - F_T b) x_2 \dots \right) \quad (2)$$

The coefficients  $a, b$ , and  $c$  are constants of the model and determined from the geometrical constraints. Variable  $x_2$  is the position where the angle is computed, and this is set to be the friction surface ( $x_2 = b$ ). The forces  $F$  are real-time input parameters from the sensor values of the AUT. The geometrical relations and dimensions are given in Figure 9.

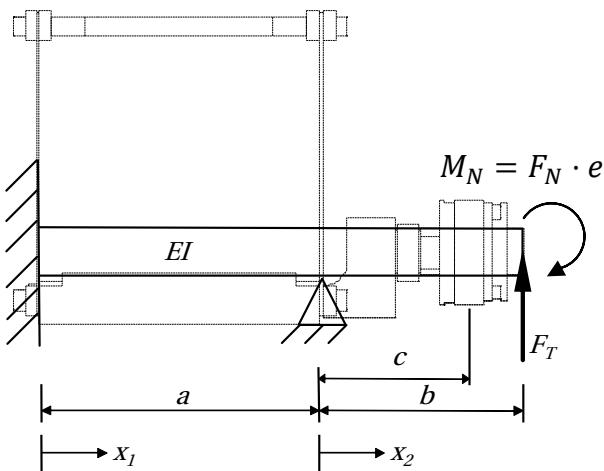


Figure 9: Geometrical dimensions of the basic beam model

The remaining constants for the material stiffness  $EI$  and the eccentricity  $e$  cannot be determined based on measurements since they represent only the analogous model. Besides, the friction

surface angle cannot be determined under load when the test specimen is in contact with the brake disc. For this reason, the procedure outlined in Figure 10 is necessary.

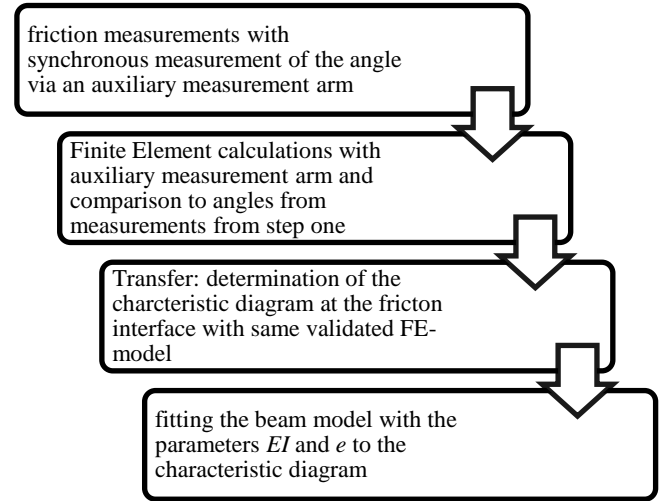


Figure 10: Procedure to determine the parameters  $EI$  and  $e$

The final parameters are found with an error minimization algorithm, reducing the final errors to under 6.6 percent for friction values below 0.67. The Observer Model is fully parameterized and can calculate the remaining angle for the control loop with a high frequency.

## 5. Performance

### 5.1. Speed-Performance

The new adaptive system can compensate for the occurring angles during friction measurements. It is faster than the AUT's linear axes, which means that delays only come from the processing of data or when the input parameters show discontinuities.

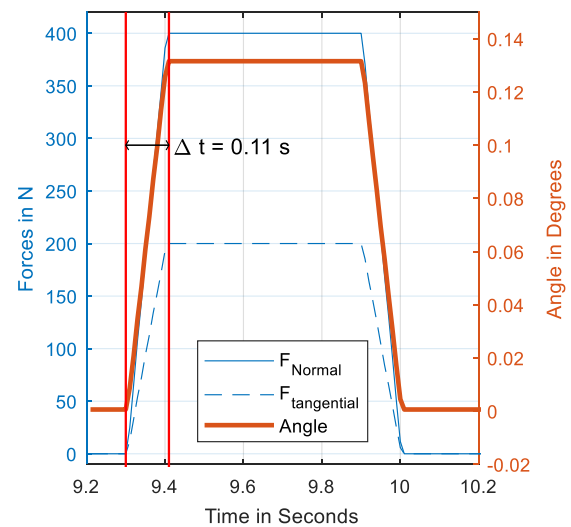


Figure 11: Friction measurement without angular compensation

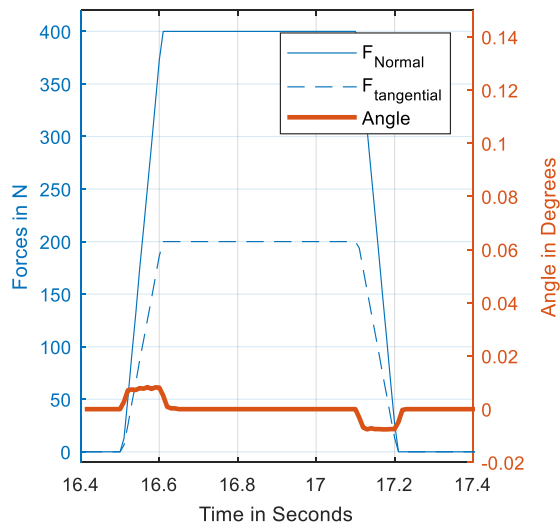


Figure 12: Friction measurement with angular compensation

Figure 11 and Figure 12 show a comparison of friction measurements with and without adaptive angle control. It is obvious, that the system intervenes quickly when the normal and tangential forces are changing, limiting the maximum angle to 1 mgrad during the adjustment process. After the input parameters settle at a steady-state, full compensation is reached within 20 ms, which is significantly shorter than the typical shortest friction test procedures ( $>1s$ ).

## 5.2. Thermal Stability

The current is continuously flowing through the stepper motor to realize the holding torque. The losses in the motor convert electrical energy to heat, which can shorten the life cycle of the electric components. Active convection cooling, e.g. a fan, is not applicable for wear and emission measurements since they can be influenced by the turbulent airflow close to the friction interface. To stabilize the motor temperature below 50 °C, a water cooling system with an external fan is used. Extensive friction procedures with applied driving profiles from real-world vehicle tests [13] were investigated to prove the effectiveness of the cooling system.

## 5.3. Interaction with Applied Normal Force

Due to its horizontally moving design [7], the prototype had a direct influence on the normal force when the angle was adjusted. This effect is addressed with the exclusive vertical movement of the new adaptive system. A change in angle is only visible in the normal force to a very small extent, for maximum normal load and maximum adjustment, it is below 1.4 %. Besides, the motor is powerful enough to realize the desired loads and speeds even under full load from the tribological contact.

## 6. Conclusion

Deflections under load are inevitable and present in any technical system, and pin on disc testers are extraordinarily sensitive to this. The challenge is to compensate those angles dynamically during friction measurements fast enough to keep the influences on the tribological contact as small as possible. The result is an adaptive compensation modification to the existing load unit of the AUT,

which is sensing the residual angle of the test specimen and controlling it. Even under dynamic changes of forces and speeds, it is capable of realizing a full surface contact (Figure 13). Detailed friction measurements with the adaptive system are presented in [12].

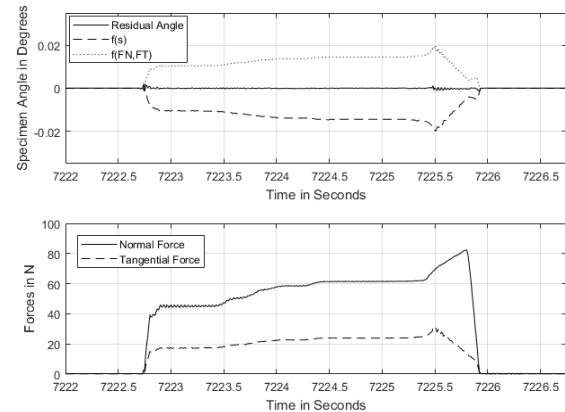


Figure 13: Result of the adaptive compensation under dynamic measurement scenarios

The adaptive enhancement to the AUT enables confident and fast short-term measurements of wear and emissions. The implemented water cooling system, which is not disturbing any particle sensors or wear measurement devices or distorting the surfaces itself achieves a high resilience.

## References

- [1] Ostermeyer, G.-P.: Friction and wear of brake systems. In: *Forschung im Ingenieurwesen* 66 (2001), 01, S. 267–272.
- [2] Ostermeyer, G.-P., Kijanski, J.: Surface Reservoir Dynamics in Friction Interfaces, Proc. EuroBrake 2019, Dresden, EB2019-FBR-022
- [3] Ostermeyer, G.-P.; Schramm, T.; Raczek, S.; Bubser, F.; Perzborn, N.: The Automated Universal Tribotester. In: FISITA (Hrsg.): Eurobrake 2015 Proceedings. Dresden: Fisita, 2015, S. 4–6. – EB2015-STQ-016
- [4] Raczek, S., Ostermeyer, G.-P.: On the Software Development for a Reduced Scale Brake Dynamometer, Proc. EuroBrake 2016, Mailand, EB2016-SVM-056
- [5] Schramm, T. and Ostermeyer, G.-P.: Measurement of surface dynamics, Proc. EuroBrake 2017, Dresden, EB2017-FBR-001
- [6] Ostermeyer, G.-P. and Vogel, A.: Principal Measurement Inaccuracies of Pin-on-Disc Testers and Associated Mitigation Efforts. In: SAE Technical Paper (2017). – 2017-01-2497
- [7] Vogel, Alexander and Ostermeyer, G.-P.: Adaptronic Actuator to Minimize the Pins Misalignment on Pin-on-Disc Testers. In: SAE Technical Paper, 2018
- [8] Burris, D.L. and Sawyer, W.G., “Addressing Practical Challenges of Low Friction Coefficient Measurements”, *Tribology Letters* 35, 2009.
- [9] Sidebottom, M.A. and Krick, B.A., “Transducer Misalignment and Contact Pressure Distributions as Error Sources in Friction Measurement on Small-Diameter Pinon- Disk Experiments”, *Tribology Letters*, 2015.
- [10] Garcia-Prieto, I., Faulkner, M.D., and Alcock, J.R., “The Influence of Specimen Misalignment on Wear in Conforming Pin on Disk Tests,” 2004.

- [11] Schmitz, T.L., Action, J.E., Ziegert, J.C., and Sawyer, W.G., “The Difficulty of Measuring Low Friction: Uncertainty Analysis for Friction Coefficient Measurements”, *Journal of Tribology* 127, 2005.
- [12] Ostermeyer, G.-P. and Vogel, A.: On Short-time Measurements of Friction and Wear with a Self-adjusting Pin-On-Disc Tester. Eurobrake 2020, EB2020-FBR-034, Barcelona, Spain
- [13] Kijanski, J., Otto, J., Lehne, G., Tiedemann, M., Ostermeyer, G.-P.: Prediction of Brake Pad Wear based on real Driving Profiles using a Pin-on-Disc Tribotester. Eurobrake 2020, EB2020-FBR-036, Barcelona, Spain